Strategy to Avoid Over-Voltages in Long Distance Driving of Induction Motors

Edson A. Vendrusculo e José A Pomilio
School of Electrical and Computer Engineering
State University of Campinas - UNICAMP
C.P. 6101, CEP 13081-970, Campinas, Brazil
{adriano,antenor@dsce.fee.unicamp.br}

Abstract - **A long distance driving system of an induction motor is analyzed with regarding to the over-voltage phenomena. The oil exploitation performed in sea deep water is a typical case, where the overall system is comprised of an inverter, a step-up transformer, a long cable and a motor. The transformer use depends on the distance and power level employed. Due to resonance between system's components one critical frequency range can be identified in which high frequency components produced by the inverter switching must be avoided. A strategy based on the inverter switching-frequency change is suggested as an alternative to minimize the over-voltage as well the inverter output current. The switching frequency choice can be performed taking into account the voltage transfer function and the input impedance of the system. The system parameters, needed for the frequency response analysis, are taken from observing the current waveform in the time domain at the inverter output.**

I. INTRODUCTION

Long distance driving of induction motors (IM) has received special attention in the last years [1-4]. The distance between the driver and the motor varies between a few tens of meters up to tens of kilometers. The last case is typical of sub-sea oil exploitation [5], while the former is common in industrial plants.

Problems that arise in these situations are related with resonance phenomena due to the long power cable. Most of the IM industrial drivers are based on PWM inverters. It is well know that the broad PWM signal spectrum can easily excite some of the system's resonance frequencies, thus over-voltages and over-currents will appear in the system, either at the motor end or along the cable [6]. Obviously, if a low-frequency purely sinusoidal signal is applied to the system, no resonance will be excited. However such a driver would need power filters or topologies that are more sophisticated (like multilevel), increasing its cost and complexity. If a PWM driver could generate an output that did not excite the resonance, the system behavior would be similar to that obtained in usual systems with short leads.

This paper discuss about choosing the PWM switching frequency that encompass the lesser over-voltage and over-current subjection to the system. Naturally, it is looked up for a PWM signal which spectrum does not coincide with the system main resonance frequency. This specific frequency is assigned since it is usually close to the inverter frequency switching.

II. THE SYSTEM

In this section, a method to estimate the parameters of the long-distance driving system components is discussed. It is done looking for identifying the oscillation in the inverter output current waveform due to the resonance phenomena. Usually, due to the high power level needed in oil exploitation applications, a step-up transformer is connected at the inverter output. Fig. 1 shows the long distance driving system. Therefore, in order to generalize this study both systems, provided with and without a transformer, are treated. The latter is characteristic of industrial plants.

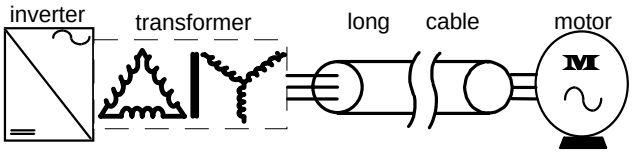

Fig. 1. The long distance driving system.

A. Identification of the System Parameters

The system parameters are identified observing the inverter output current. Despite the voltage at the motor leads could also be used, the current is preferred since the motor leads may not be physically available. Commonly, the motor is located far away from the inverter as well as sometimes in a inaccessible place.

1) Inverter - Cable - Motor (ICM) System

In this system the over-voltage phenomenon occurs due to the cable's natural frequency (f_o). It has been widely disclosed in the literature [2]. This frequency can be measured from the inverter output current waveform when the cable is excited by a PWM voltage inverter, as showed in Fig. 2. This typical source provides a sequence of voltage steps and the resultant oscillation observed at the current signal is only dictated by the cable characteristics itself [2]. Thus, the cable parameters can be determined from the cable's frequency as follow [7].

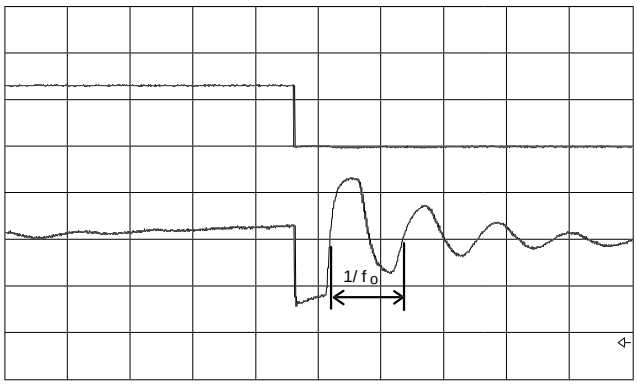

Fig. 2. System's waveforms at the inverter output, top: Voltage (250V/div); Bottom: Current (2A/div). Horizontal scale: 25μs/div.

The capacitance between two cable conductors, per unit length, is given by:

$$C_C = \frac{5.10^4 \pi}{\cosh^{-1}\left(\frac{d}{2r}\right).(lf_O)^2}\left[\frac{\mathrm{F}}{\mathrm{m}}\right], \quad (1)$$

where r is the radius, d is the separation distance between the cable conductors and l is the cable length. The conductance may be written immediately from an inspection of the capacitance expression,

$$G_C = 2.10^{-5}\sigma(l.f_O)^2 C_C\left[(\Omega\mathrm{m})^{-1}\right]. \quad (2)$$

The conductivity of the dielectric is approximately $\sigma \cong 10^{-9}$ mhos/m, considering the material commonly used either polyethylene or polypropylene. The inductance of one conductor is:

$$L = \frac{1}{C_C.(4lf_O)^2}\left[\frac{\mathrm{H}}{\mathrm{m}}\right]. \quad (3)$$

These equations are valid to the electromagnetic fields outer of the cable conductors. No piece of information about the Skin effect is included. Furthermore, the above equations are valid to systems where the inverter output voltage risetime is less than the time spent to the voltage pulse reach the motor end of the cable [2].

2) Inverter - Transformer -Cable - Motor (ITCM) System

With the transformer in the system, the over-voltage phenomenon makes up due to a series resonance. This resonance is dictated by the interaction between half of all cable inductance plus the transformer leakage inductance and all cable capacitance [6]. Summarizing, the transformer leakage inductance is algebraically given by:

$$L_{tr} = \left(\frac{1}{(2\sqrt{2}f_r\pi)^2 C_C.l} - \frac{L.l}{4}\right)[\mathrm{H}], \quad (4)$$

where f_r is the resonance frequency that can be measured in the inverter output current as showed in Fig. 3. Like the ICM system, this frequency can be directly measured from the current waveform observation.

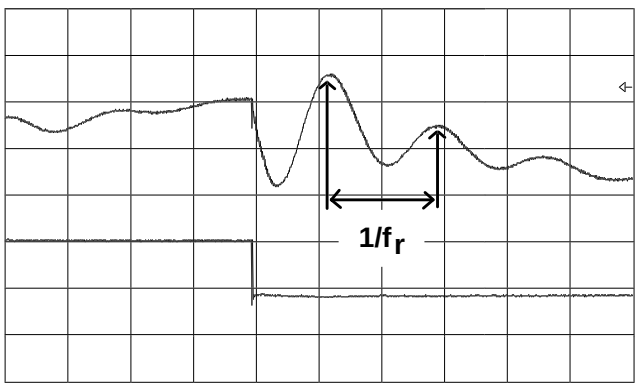

Fig. 3. System's waveforms at the inverter output, top: Current (1A/div); Bottom: Voltage (50V/div). Horizontal scale: 50μs/div.

Note that the cable parameters are necessary to have the leakage inductance determined. To overcome this matter, a voltage step could primarily be applied to the cable, in order to have the cable parameters determined. To this turn, no disconnection of the transformer is necessary.

The other parameters of the step-up transformer as the winding resistance (R_{tr}) and magnetization inductance (L_{otr}) can be obtained from pattern tests or manufacturer information. It is assumed that these two parameters are related to a single phase transformer model with respect to the high voltage side (Y connection in Fig. 1). The leakage inductance calculated from (4) is already computed relative to this side.

III. SYSTEM FREQUENCY RESPONSE

In this section, the frequency response of the system is analyzed. All results were performed using the frequency domain model disclosed in [6]. Regarding to the motor over-voltage and inverter over-current limits the voltage transfer function and the system input impedance are respectively analyzed. These functions describe the ratio between the motor and inverter voltages and the ratio between the inverter voltage and current, respectively. The cable parameters and the transformer leakage inductance were estimated as indicated in section II-A.

A. ICM System

The frequency response is performed by the system modeling disclosed in [6]. It has been showed that the voltage transfer function can be expressed by:

$$G_V = \frac{1}{\cosh(\gamma.l)}, \quad (5)$$

where γ is the propagation constant for transmission line cables defined as:

$$\gamma = \sqrt{\left\{\frac{3}{2}.R_{hyp} + j\omega(L_{hyp} + (L - 50e-9))\right\}.\{G + j\omega C_C\}}, \quad (6)$$

where ω is the frequency. The skin effect of the conductor parameters are taken into account using the hyperbolic terms (R_{hyp} and L_{hyp}) [7]. Traditionally, the skin effect has been assigned using Bessel functions. However, these functions are computationally hard so that hyperbolic approximations were preferred. Within acceptable accuracy these approximations are related to:

$$R_{hyp} = \frac{1}{\pi r\sigma\delta}\left(\frac{\mathrm{senh}\frac{2r}{\delta} + \mathrm{sen}\frac{2r}{\delta}}{\cosh\frac{2r}{\delta} - \cos\frac{2r}{\delta}}\right)\left[\frac{\Omega}{\mathrm{m}}\right], \quad (7)$$

$$L_{hyp} = (75e-9).\frac{\delta}{r}\left(\frac{\mathrm{senh}\frac{2r}{\delta} - \mathrm{sen}\frac{2r}{\delta}}{\cosh\frac{2r}{\delta} - \cos\frac{2r}{\delta}}\right)\left[\frac{\mathrm{H}}{\mathrm{m}}\right], \quad (8)$$

where σ is the conductivity to the conductor material (for cooper σ=5.75e7 $[\Omega\mathrm{m}]^{-1}$) and δ is the skin depth of penetration, which is frequency dependent as:

$$\delta = \sqrt{\frac{2}{\sigma\mu_C\omega}}\ [m], \quad (9)$$

to material of the conductor with permeability μ_c (it means 4 πe-7 for cooper) . The system input impedance is calculated as:

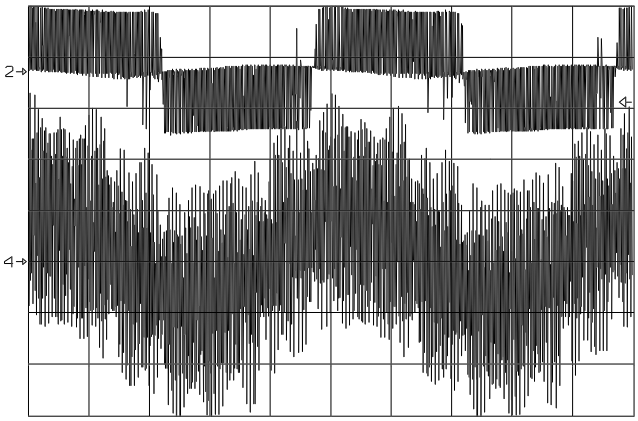

Fig. 9. Inverter voltage (50V/div - top); Motor voltage (50V/div - bottom). Horiz.: 10ms/div.

These waveforms are produced by using a 1.55kHz switching frequency as seen in Fig. 10.

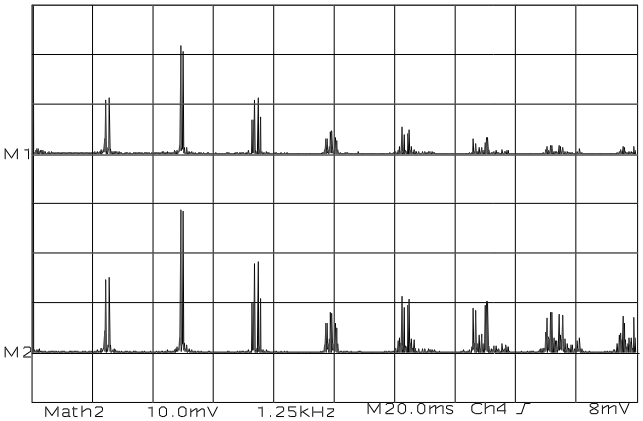

Fig. 10. Frequency spectrum: Inverter voltage (5V/div - top); Motor Voltage (5V/div - bottom). Horiz.:1.25kHz/div.

It is clear analyzing the motor voltage spectrum that the over-voltage observed in Fig. 9 is due to the amplification of some PWM harmonics. To highlight the amplification effect, the switching frequency was set equal 11.2kHz, the resonance frequency of the ITCM system is shown in Fig. 11.

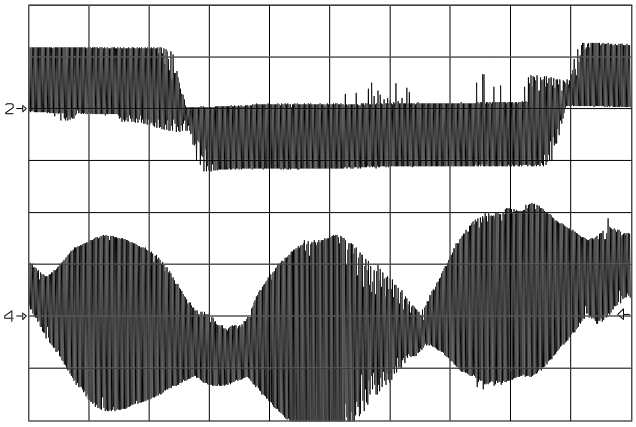

Fig. 11. Inverter voltage (50V/div - top); Motor voltage (50V/div - bottom). Horiz.: 4ms/div.

In this situation, a motor stress greater than 2 p.u. is observed. The experimental frequency response (Fig. 8) predicts the amplification to be 5 times at the resonance frequency as evidenced in Fig. 12

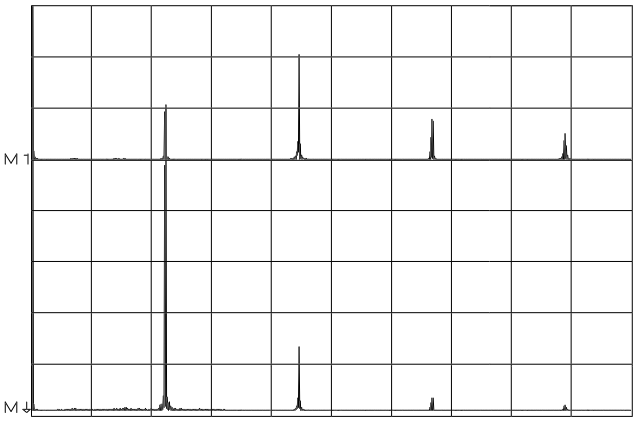

Fig. 12. Frequency spectrum: Inverter voltage (5V/div - top); Motor Voltage (5V/div - bottom). Horiz.:5kHz/div.

Clearly, harmonics amplification are strongly related to the voltage transfer function (Fig. 8). Finally, to the switching frequency set to 21kHz the over-voltage was eliminated as showed in Fig. 13.

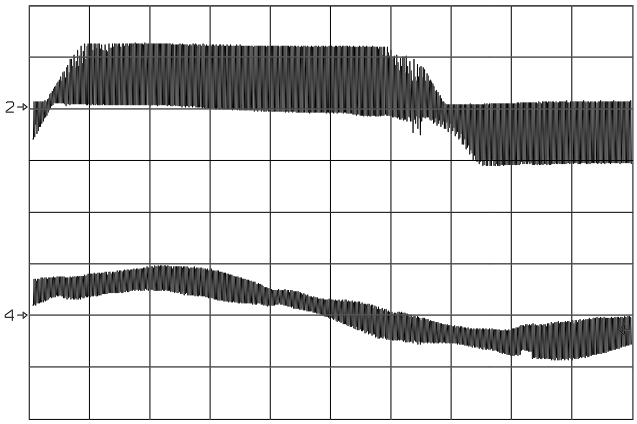

Fig. 13. Inverter voltage (50V/div - top); Motor voltage (50V/div - bottom). Horiz.: 4ms/div.

According to the experimental voltage transfer function, the magnitude of PWM harmonics are in Fig. 14.

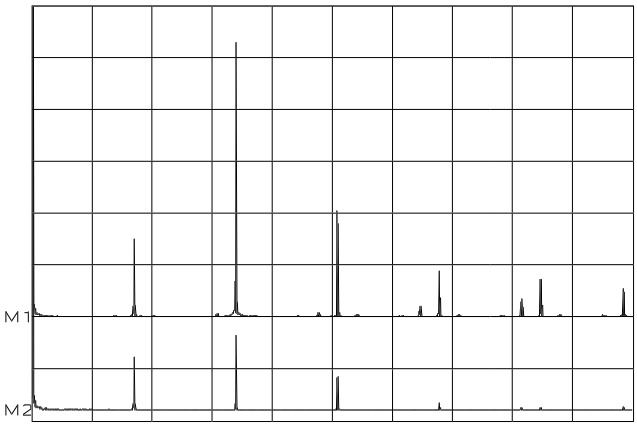

Fig. 14. Frequency spectrum: Inverter voltage (2.5V/div - top); Motor Voltage (2.5V/div - bottom). Horiz.:12.5kHz/div.

With regard to the input impedance, the inverter output

$$Z_{sys} = Z_C \frac{1}{\tanh(\gamma.l)}, \tag{10}$$

where the characteristic impedance (Z_c) of the transmission line cable is given by:

$$Z_C = \sqrt{\frac{\left\{\frac{3}{2}.R_{hyp} + j\omega(L_{hyp} + (L - 50e - 9))\right\}}{\{G + j\omega C\}}}. \tag{11}$$

Fig. 4 shows the results obtained by simulation of an actual system with the following cable parameters:
Cable → length = 8km; conductors area = 34 mm^2; L=360µH/km ; Cc=160nF/km ; G=100nmhos/km.

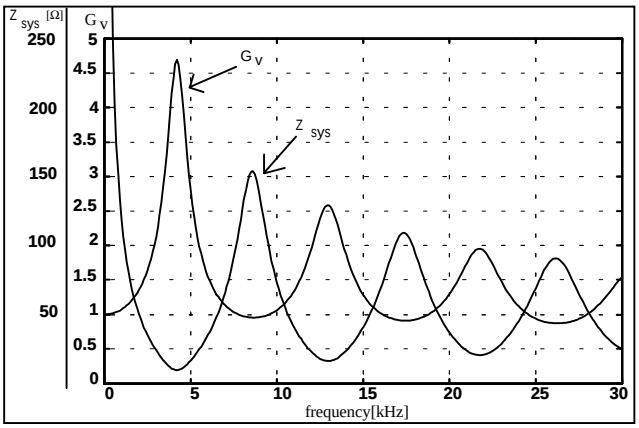

Fig. 4. Voltage transfer function (G_v) and input impedance (Z_{sys}) of an actual ICM system.

For safe system operation, G_v and Z_{sys} behavior can be used to predict the system response to the harmonics injected by PWM voltage source inverter. Firstly, the analyze could be done through simple observation to avoid matching the PWM spectrum with system resonance. Nevertheless, a suggestion to choose the inverter switching frequency will be presented later, based on the current and voltage limits.

B. ITCM System

Introducing the transformer, the voltage transfer function is now rearranged to (12) and (13) [6]. These equations were deduced considering high power applications systems. It is a typical situation in sub sea oil exploitation where the motor power is rate to dozens of kVA. It is important to highlight that the skin effect in the transformer winding is not taken into account in (12) and (13). This is unnecessary since in high power systems the cable is long enough in such way that its parameters are dominant over the transformer ones. Therefore, the attenuation is mainly dictated by the cable. Fig. 5 shows the frequency response to this kind of system.

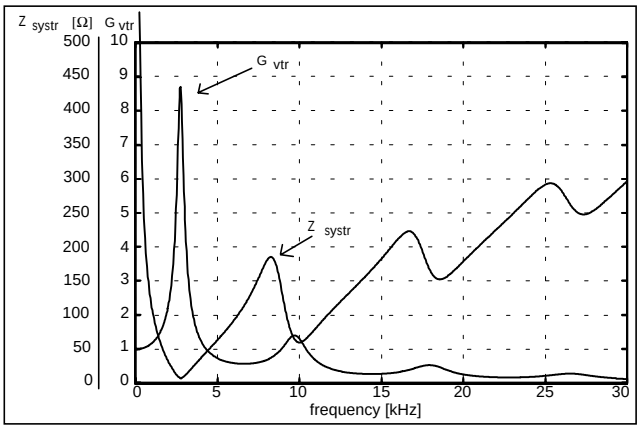

Fig. 5. Voltage transfer function (G_{vtr}) and input impedance (Z_{systr}) of an actual ITCM system.

The power transformer parameters were:
Power Transformer (150kVA) → R_{tr}=63mΩ ; L_{tr}=806µH ; L_{otr}=2,93H.

IV. INVERTER SWITCHING FREQUENCY CHOICE

Considering safe operating limits for motor over-voltage and inverter over-current, the detailed system frequency response is used to choose the more suitable inverter switching frequency. In a first step, the switching frequency should be higher than the resonance frequency determined considering the system parameters as in section II.A.

A method to find more precisely this frequency is proposed. Since the voltage transfer function and the system input impedance behavior are traced from transcendental equations, a numerical method has been applied in order to determine the switching frequency to reach a voltage gain specified by the user. It can be accomplished using the secant numerical method. The numerical method is applied to the voltage transfer function curve in the spectrum region with its extremes delimited by the resonance (ITCM) or cable's oscillation (ICM) frequency and the frequency correspondent to the first valley. Holding the obtained frequency value, the inverter current charging can be readily verified through observing the input impedance response.

$$G_{vtr} = \frac{Z_C . j\omega L_{otr}}{Z_C\{R_{tr} + j\omega(L_{tr} + L_{otr})\}\cosh(\gamma.l) + \left((j\omega L_{tr} + R_{tr})^2 + j2\omega L_{otr}(j\omega L_{tr} + R_{tr})\right).\mathrm{senh}(\gamma l)} \tag{12}$$

$$Z_{systr} = \frac{Z_C\{R_{tr} + j\omega(L_{tr} + L_{otr})\}\cosh(\gamma.l) + \left((j\omega L_{tr} + R_{tr})^2 + j2\omega L_{otr}(j\omega L_{tr} + R_{tr})\right).\mathrm{senh}(\gamma l)}{Z_C\cosh(\gamma.l) + \{R_{tr} + j\omega(L_{tr} + L_{otr})\}\mathrm{senh}(\gamma l)} \tag{13}$$

V. DIGITAL SIMULATION AND EXPERIMENTAL VERIFICATION

Following, simulations and experimental results of a prototype system as showed in Fig. 1, are presented. The parameters were determined as proposed in this paper. The period oscillation at the inverter current (Fig. 2) is 29.8 μs that results in 33.5kHz cable's natural oscillation frequency. The cable presents 990 m length with conductors of radius r=1.12mm (area=4mm^2) and center-to-center separation d=4.62mm. The capacitance, found by (1), is C_c=106pF/m. From (2) and (3), the conductance and inductance are G_c=2.33nmhos/m and L=534.6nH/m, respectively. Regarding to the transformer, the measured resonance frequency is 11.2kHz (Fig. 3) and the leakage inductance, L_{tr}=818.4μH from (4). The winding resistance, R_{tr}=2.9Ω and the magnetization inductance $Lotr$=6.4H were measured for the single phase transformer model using pattern tests and values referred to the high voltage side.

A. ICM System

Fig. 6 shows the voltage transfer function of the ICM system (G_v) obtained from (5) and the experimental values measured with a HP Dynamic Signal Analyzer 35660A.

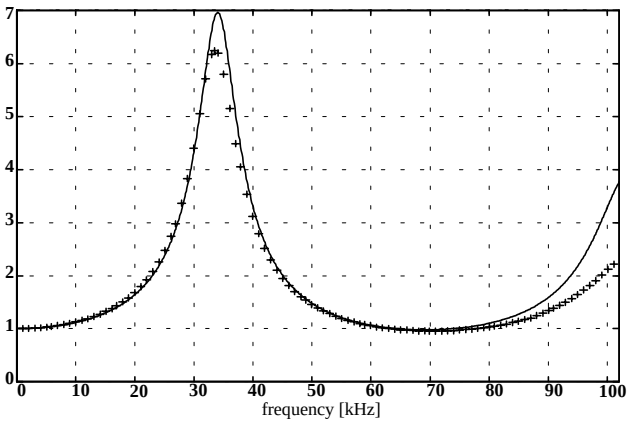

Fig.6. Voltage transfer function of an ICM system: digital simulation (solid) and experimental (+ dot).

The waveform peak occurs at the 33.5kHz cable's natural oscillation frequency in agreement with voltage step response pointed out in Fig. 2. The simulated attenuation presents some difference from experimental results, mainly in the high frequency range. Fig. 7 shows the correspondent input impedance of the system.

Again, the curves present some divergence in the high frequency range what can be due to the error introduced by using hyperbolic functions rather than Bessel functions to take into account the skin effect.

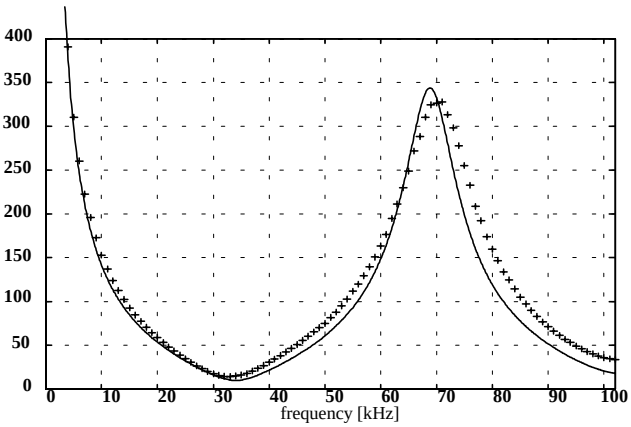

Fig.7. Input impedance of an ICM system: digital simulation (solid) and experimental (+ dot).

B. ITCM System

To this system a rated apparent power of 0.8kVA and rated voltage of 150Δ-220Y step-up transformer was used. In this prototype system the skin effect significantly affects the transformer parameters in respect to the cable ones, unlike assumed by deducing (12) and (13), therefore only experimental results are presented in Fig. 8.

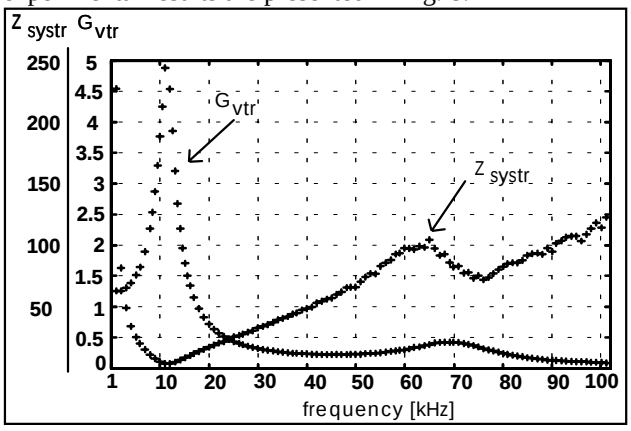

Fig.8. Voltage transfer function (G_{vtr}) and input impedance (Z_{systr}) of an ITCM system: experimental results.

These curves were used to choose the switching frequency. Using the secant numerical method applied to the voltage transfer function, and establishing an allowed over-voltage lower than unit, the 21kHz switching frequency was determined. Following experimental results for switching frequencies lower and equal to the resonance one, as well as at 21kHz are showed.

C. Effects of Changing the Switching Frequency

The experimental results in the time domain considering different frequencies when exciting the ITCM system are as follow. Fig. 9 shows the over-voltage effect.

current is shown in Fig. 15.

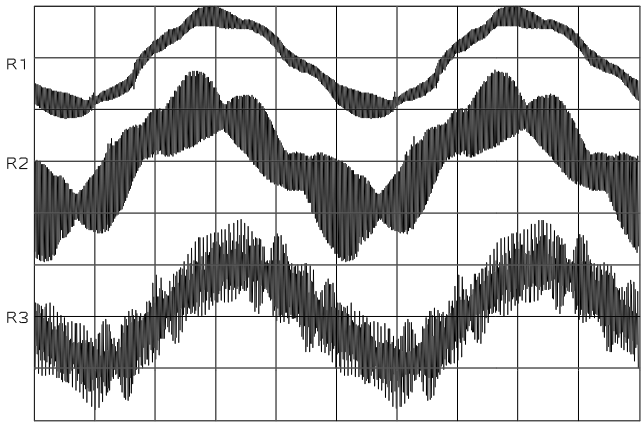

Fig. 15. Inverter output current depending on the switching frequency (1A/div). At top: 21kHz. Medium: 11.2kHz. Bottom: 1.5kHz. Horiz.: 10ms/div.

Naturally, the current ripple decreases as much as the frequency grows up characterizing the input impedance behavior predicted by the frequency domain analysis.

VI. CONCLUSIONS

Systems composed by induction motors fed by PWM inverters through long cables are subject to over-voltage caused by resonance phenomena. The system's main resonance-frequency was well characterized as cause of motor over-voltages. The motor over-voltage was extinguished by setting the PWM-driver switching-frequency higher than the resonance frequency. With acceptable accuracy the switching frequency can be chose using the system frequency response characteristics.

A set of equations allows to predict the system behavior for a wide frequency range. However, the equations respect to the ITCM system are valid only to power systems of kVA power range or higher. The system parameters are estimated through straightly observing the oscillation at the inverter output current to both ICM and ITCM system. Despite of the study had been developed aiming sub sea oil exploitation applications, the overall results are useful tool for understanding the over-voltage phenomena and can be readily used to motor safe operation when installing adjustable speed drivers in industrial plants.

VII. ACKNOWLEDGMENT

The authors wish to acknowledge the financial support of the FAPESP (Fundação de Amparo à Pesquisa do Estado de São Paulo), under Project Number 96/01375-0 and the contributions of Prof. Lourenço Matias.

VIII. REFERENCES

[1] Persson, E., "Transient Effects in Application of PWM Inverter to Induction Motors", *IEEE IAS Transaction*, vol. 28, nº 5, Sept./Oct. 1992.

[2] Skibinski, G.; Leggate, D.; Kerkman, R. J., “Cable Characteristics and Their Influence on Motor Over-Voltages”, *IEEE APEC Conf. Proc.*, pp.114-120, Feb. 1997.

[3] Jouanne, A. von; Enjeti, P.; Gray, W., “The Effect of Long Motor Leads on PWM Inverter Fed AC Motor Drive Systems”, *IEEE APEC Conf. Proc.*, pp.592-597, March 1995.

[4] de Lima, A. C. S.; Stephan, R. M.; Pedroso, A.; Mourente, J., "Analysis of a Long Distance Drive for an Induction Motor", *ISIE'96 Proc.*, pp. 867-872, June 1996.

[5] Raad, R. O.; Henriksen, T.; Raphael, B. H.; Hadler-Jacobsen, A., “Converter-Fed Subsea Motor Drives”, *IEEE Trans. Ind. Applicat.*, vol 32, no.5, pp. 1069-1079, Sept./Oct. 1996.

[6] Pomilio, J. ª; Souza, C.R.; Matias, L., Peres, P. L. D.; Bonatti, I. S., “Driving AC Motors through a Long Cable: The Inverter Switching Strategy”, *IEEE-International Electrical Machine Drives Conference – IEMDC’97*, pp. MB1-4.1-MB1-4.3, Millwauke, May 1997.

[7] Vendrusculo, E. A.; Pomilio, J. A., "Power Cable Parameters Estimation in Long Distance Driving of Electrical Machines", *IEEE International Electrical Machines and Drives Conference - IEMDC'99*, pp. 410-412, May 1999.